DARU Journal of Pharmaceutical Sciences (2023) 31:119–133
https://doi.org/10.1007/s40199-023-00467-x

RESEARCH ARTICLE

In silico screening, synthesis, characterization and biological evaluation of novel anticancer agents as potential COX-2 inhibitors

Ankita Sahu[1] · Dibyabhaba Pradhan[2] · Babita Veer[3] · Sumit Kumar[1] · Ram Singh[3] · Khalid Raza[4] · Moshahid A. Rizvi[5] · Arun Kumar Jain[6] · Saurabh Verma[1]

Received: 6 January 2023 / Accepted: 12 June 2023 / Published online: 15 July 2023

Abstract

Background Cyclooxygenase enzyme is frequently overexpressed in various types of cancer and found to play a crucial role in poor prognosis in cancer patients. In current research, we have reported the new COX-2 inhibitors for cancer treatment using computer-aided drug design and experimental validation.

Methods A total of 12,795 compounds from the different databases were used to screen against the COX-2 enzyme. It perceived three new compounds with better binding affinity to the enzyme. Afterwards, physicochemical properties and *in silico* bioactivity were assessed for efficacy, safety, and structural features required for binding. The molecules were synthesized and confirmed by spectroscopic techniques. Later on, molecules were evaluated for their anti-cancer activity using MCF-7, MDA-MB-231 and SiHa cancer cell lines.

Results Compound ZINC5921547 and ZINC48442590 (**4a**, and **4b**) reduced the MCF-7, MDA-MB-231, and SiHa cells proliferation potently than parent compounds. The PG-E2 estimation shown, both compounds act through the COX-2 PGE2 axis. Compound **4a** and **4b** block the cell cycle at G1-S phase and induce cancer cell death.

Conclusions We concluded that compounds **4a** and **4b** effectively promotes cancer cell death via COX-2 PGE2 axis, and further *in vivo* studies can be evaluated for development in both compounds as anticancer agents. The compilation of this information will help us to generate better outcome through robust computational methods. The high-quality experimental results may pave the way for identifying effective drug candidates for cancer treatment.

Keywords COX-2 receptor · Molecular docking · ADMET properties · Synthesis · MTT assay · Apoptosis

✉ Saurabh Verma
svarmasv1@rediffmail.com; saurabhverma.nip@gov.in

Ankita Sahu
ankitasahumbt@gmail.com

Dibyabhaba Pradhan
dbpinfo@gmail.com

Babita Veer
babita.veer28@gmail.com

Sumit Kumar
sumitguptabt@gmail.com

Ram Singh
ramsingh@dtu.ac.in

Khalid Raza
kraza@jmi.ac.in

Moshahid A. Rizvi
mrizvi@jmi.ac.in

Arun Kumar Jain
drakjain@gmail.com

[1] Tumor Biology, ICMR-National Institute of Pathology, New Delhi 110029, India

[2] Indian Biological Data Center, Regional Centre for Biotechnology, Faridabad 121001, India

[3] Department of Applied Chemistry, Delhi Technological University, New Delhi 110042, India

[4] Department of Computer Science, Jamia Millia Islamia, New Delhi 110025, India

[5] Department of Bioscience, Jamia Millia Islamia, New Delhi 110025, India

[6] Biomedical Informatics Centre, ICMR-National Institute of Pathology, New Delhi 110029, India

Introduction

Cyclooxygenase (COX) is widely known as a critical target protein for targeting various cancers. It belongs to the family of isozymes, EC 1.14.99.1, also referred to as prostaglandin-endoperoxide synthase (PTGS). There are two known isoforms of COX-2 (COX-1 and COX-2), homodimer with 71 KDa monomeric unit. This enzyme is responsible for the baseline level formation of prostanoids, including thromboxane and prostacyclin [1, 2]. It catalyzes the conversion of arachidonic acid to prostaglandins (PGs), which play a significant role in cancer cell proliferation and cell death [3–5]. Overexpression of COX-2 targeted protein is associated with precancerous lesion, cancer initiation and progression [6, 7]. It has been found in different multiple cancer types including breast, ovarian, melanoma, glioblastoma, prostate etc. [3, 8, 9]. The treatments of cancer are challenging due to its heterogenicity, high recurrence, and high mortality rate causing millions of cancer-related deaths worldwide [10–12]. The new approach emphasizes primarily identifying active molecules for the COX-2 enzyme-containing noteworthy activity in cancer treatment.

COX-2 expression in primary breast cancer has been observed in nearly 40% of patients at both pre-invasive and invasive stages of the disease [13]. In addition, the expression is significantly associated with breast cancer progression and is stimulated by different growth factors, tumor promoters, cytokines, mitogens, hormones and prostaglandins which are associated with inflammatory processes and are seen as a prognostic factor in cancer development and progression [14–16]. Upregulation of cyclooxygenase-2 (COX-2) in human cancers has been demonstrated in limited studies including in breast carcinomas, human colorectal cancers, colon cancer, prostate adenocarcinomas, gastric adenocarcinoma, and adenoma, in head and neck cancer [9]. In view of the above facts, COX-2 has been the cause to induce angiogenesis in various types of tumors and it is a target of COX-2 inhibitors for therapeutic use [9, 17, 18].

Conceptually, NSAIDs prevent cancer through their effects on the eicosanoid pathways. COX-2 inhibitory drugs show protective effects in breast cancer. Some studies reported that Triple Negative Breast Cancer (TNBC) and COX-2 expression are associated with worse outcomes in early and locally advanced breast cancer patients due to large tumor size and higher grade are associated with ER-/PR-negative [19, 20]. Since, human cancers have elevated PGE_2 levels (most abundant prostaglandin) and its inhibition associated with the tumor development and progression.

A large number of chemicals are difficult to carefully test and evaluate. Instead, standard toxicity testing and applying computational methods have been limited to only a small number of chemicals. Based on the *in silico* investigation, three new compounds were selected and evaluated the anticancer activities followed by chemical evaluation. Multiple computational studies, *in vitro* and *in vivo* studies have been supported the notion that COX-2 has utility against many forms of cancers [9, 21]. The computer-aided drug design (CADD) approach made it possible to identify new potential inhibitors against a target of interest [22]. Precise treatment of individual components is pivotal to calculating the binding free energies. Computational methods have been used for identifying potential drug molecules for the targeted protein [23]. We highlighted the identification of COX-2 inhibitors that were subjected to further *in vitro* validations for the treatment of breast cancer.

Identification of new compound analogs with improved solubilities and activities, a series of fenamates N-substituted anthranilic acid derivatives were designed and synthesized based on the *in-silico* outcomes. The fenamates non-steroid anti-inflammatory drugs (NSAIDs) are extensively chosen for the treatment of pain, fever, and inflammation [24, 25] and also have shown an effect on cancer prevention [26]. In most cancer cases, the expression level of COX-2 is directly proportional to tumour growth. Most classes of Fenamates are the utmost potent NSAIDs COX-2 inhibitors [24]. Several studies found that NSAIDs are capable to inhibit cancer proliferation via suppressing angiogenesis, metastasis and regulating several apoptosis-related signalling pathways[27]. Some of the fenamates N-substituted anthranilic acid derivatives show the potential starting point for the identification of new candidates for anticancer agents, promising pharmacological and therapeutic medicines [28].

Fenamates are a subgroup of NSAIDs that is the close isosteric analogue of salicylic acid and are promising therapeutic medicines against breast cancer[26]. Based on *in-silico* outcomes, mefenamic acid, tolfenamic acid and flufenamic acid were used as parental compounds that have long been used as a medicinal agents and are deemed safe [24, 29]. Interestingly, these fenamates have been reported potently suppresses proliferation and induce apoptosis when tested against multiple breast cancer cell lines [26, 30–33]. However, the detailed efficacy and mechanisms of these derivatives as anti-cancer agents *in vitro* are very limited. Thus, the use of these primary agents prompted to synthesize of the desired compounds and to further confirmed the anticancer effect is plausible. Hence, in the current study, we identified the lead compounds that showed noteworthy potential in developing anticancer drugs, based on computational methods then synthesized, and *in vitro* investigated the inhibitory effect of compounds from cervical cell line SiHa cell and

human breast carcinoma cell lines such as MCF-7 and MDA-MB-231 cells line. This study also aimed to PGE-2 was also examined to test whether a reduction in cell proliferation is due to prostaglandin.

Methods

Computational studies

Protein Preparation

Computational methods using licensed software Schrodinger maestro 16.4 version and online resources were implemented to find out the best results. The 3D structure of potential COX-2 inhibitors (PDB ID: 5IKR) was imported from the Protein Data Bank (www.rcsb.org) indicated in Fig. 1. It consists only of heavy atoms and may include a co-crystallized ligand, water molecules, metal ions, and cofactors. PDB structure gives information regarding missing amino acids and their connectivity, which must be assigned. Besides this, the structure also assigns the bond orders, hydrogen and formal charges, so the initially protein preparation step is used. Optimization of protein was done at neutral pH and the structure was minimized using the optimized potential for liquid simulations (OPLS-2005) force field for refining the structure, by a heavy atom convergence threshold of 0.3Å[34]. The prepared structure was then checked for Ramachandran core values using the PROCHECK server [35].

Selection of ligands

The virtual screening of 12,795 compounds was performed using different databases with a structure similar to that of the COX-2 inhibitor. We downloaded different ligands in .smi format (1584, 10,126 and 1085 ligands) from Zinc15 (http://zinc.docking.org/) [36], ChemSpider database (http://www.chemspider.com/) [37, 38] and BindingDB database (https://www.bindingdb.org/) [39]. The databases were computationally screened by the structural similarity calculation using metrics Tanimoto coefficient (Tc) ≥ 0.70, where the two or more compounds share the same activities (similarity ≥ 0.70). These compounds were visually inspected for the possibility of their predicted binding modes. The ligands were prepared using the LigPrep module for ligand refinement to adjust the chemical correctness (protonation and chiralities), stereochemical, ring conformations and ionization variation [40, 41]. The ligands low energy was optimized using the OPLS-2005 force field and possible states were generated from pH 7.0 ± 2.0.

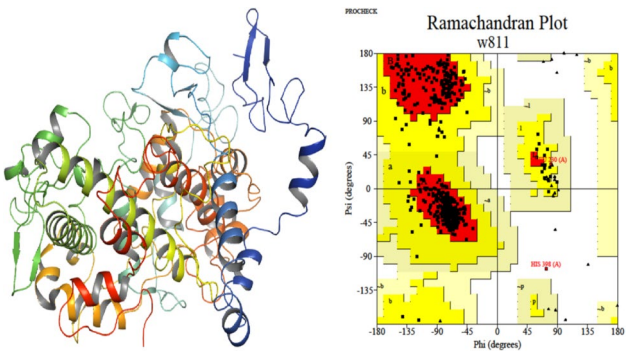

Fig. 1 Crystal structure of minimized COX-2 protein and Ramachandran Plot

Molecular docking

Grid generation was done using the receptor grid generation platform using the GLIDE (Grid-based Ligand Docking with Energetics) module of Schrodinger Suite that determines and marks the active site position [42]. In the present study, Rigid Receptor Docking (RRD) was generated at the centroid of the co-crystallized ligand to calculate the binding affinity and scores of the interactions between the target and ligands. The three-level docking methods of RRD were utilized. Docking calculations were performed using lower stringency to higher stringency through high throughput virtual screening (HTVS), standard precision (SP), and extra precision (XP) and used the default parameters [42, 43]. The XP scores are mentioned in kcal/mol, the more negative scoring gives the better binding. Therefore, the XP score improves the selection of the actual binding pose. Prime MMGBSA module is also estimated to have relative binding affinities of the ligands with the proteins [21, 44].

ADMET properties

Later, the compounds were screened for Adsorption, Distribution, Metabolism, Excretion, and Toxicity (ADMET) properties and as calculated using in silico algorithm. Qikprep module from Schrodinger maestro was used. These properties are the most challenging part of the drug development process. It predicts both physicochemical and pharmacokinetically relevant properties which influence much of the likelihood of success of the hit candidates. These properties are of prime importance for a molecule to be an active drug [45, 46]. Overall, ADMET risk provides a range between 0 and 24, where a lower value represents better draggability. The drug-likeliness of all the compounds was assessed by analysis of the pharmacokinetic profile and Lipinski's rule of five [47].

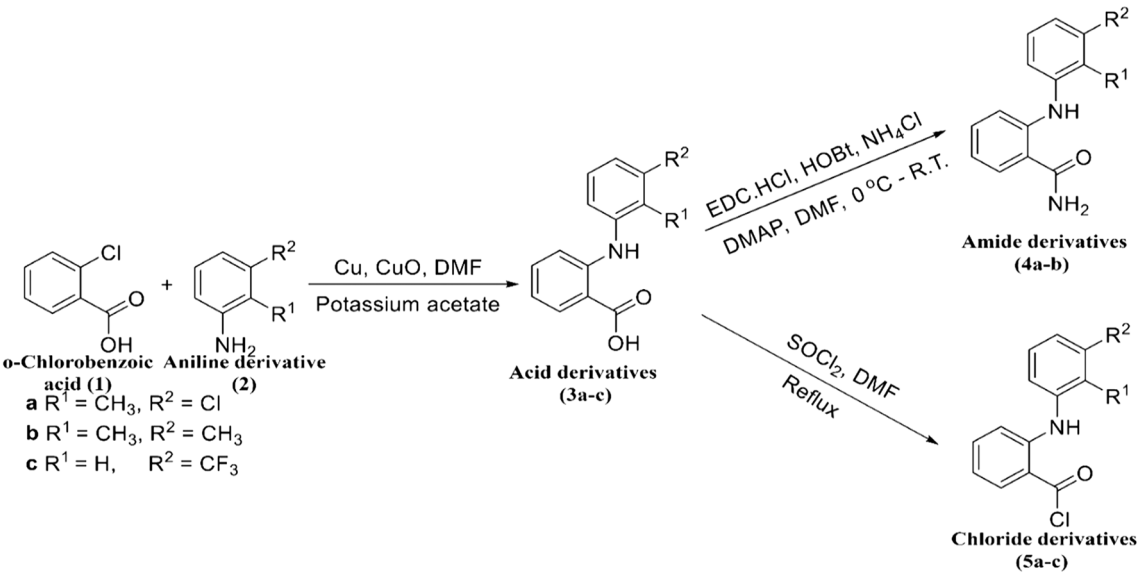

Scheme 1 Synthesis of compounds **4a-b** and **5a-c**

Chemistry evaluation

The satisfactory outcomes by *in silico* studies prompted us to synthesize the compound for further confirmation as depicted in Scheme 1.

Experimental section

General information

The purchase of all the utilized chemicals was done from commercial suppliers and used as such. 2-chlorobenzoic acid, Cu and CuO were purchased from CDH Fine chemicals and 3-chloro-2-methylaniline,2,3-dimethylaniline, and 3-(trifluoromethyl)aniline were purchased from TCI Chemicals. The progress of the reaction was monitored using TLC Silica gel 60 F_{254} plates. Melting points of the compounds were determined by the help of laboratory melting point apparatus. IR spectra were recorded on Perkin Elmer Spectrum II instrument and KBr pellet was used. ^{1}HNMR spectra of the compounds were recorded at 300 MHz and 500 MHz on Bruker NMR instrument using DMSO-d_6 as solvent. Chemical shifts δ are expressed taking TMS as internal standard. Splitting patterns are designated as singlet (S), duplet (d), triplet (t) and multiplet (m). The mass spectra of the compounds were recorded using XEVO G2-XS QTOF mass spectrometer. The elemental analysis was determined by CHNS elementar.

General procedure for synthesis of substituted 2-(phenylamino)benzoic acid (3a-c) o-Chlorobenzoic acid (1, 0.5 g, 3.1 mmol) was dissolved in DMF (4 mL) in the round bottom flask (50 mL). To this solution, Cu (0.0173 g, 0.24 mmol), CuO (0.0096 g, 0.12 mmol) and fused potassium acetate (0.3134 g, 3.1 mmol) were added slowly. The reaction mixture was vigorously stirred at 160°C for 30 min. Then aniline derivative (**2**, 3.5 mmol) was added to the above reaction mixture, and reaction was allowed to stir for 3 h. The reaction progress was monitored using TLC (benzene:ethyl acetate, 4:1). The reaction mixture cooled to room temperature and filtered after completion of the reaction using celite pad. The obtained filtrate was concentrated in vacuo and to this solution dil. HCl was added to obtain a solid product (**3a-c**).

2-((3-chloro-2-methylphenyl)amino)benzoic acid (3a): Mp. 207–209 oC (lit. mp 210-214oC)[20]; IR (KBr, cm− 1): 3401, 3339, 2857, 2644, 1655, 1581, 1498, 1431, 1261, 1164, 1010, 892, 776, 684; 1 H NMR (DMSO-d6, 300 MHz): δ 2.52 (s, 3 H, CH3), 7.05–7.11 (m, 2 H), 7.25 (t, J = 3 Hz, 1 H), 7.59–7.67 (m, 2 H), 7.75–7.80 (m, 2 H), 9.02 (s, 1 H, NH), 11.08 (s, 1 H, OH); Mass: m/z 261.0; Anal. Calcd for C14H12ClNO2: C, 64.25; H, 4.62; N, 5.35%. Found: C, 64.28; H, 4.64; N, 5.30%.

2-((2,3-dimethylphenyl)amino)benzoic acid (3b): Mp. 234–236 °C (lit. mp 230–231 °C)[21]; IR (KBr, cm^{-1}): 3398, 3109, 3045, 1659, 1567, 1501, 1489, 1257, 1131, 1022, 748, 676; ^{1} H NMR (DMSO-d6, 300 MHz): δ 2.10–2.25 (m, 6 H, CH_3), 6.98–7.05 (m, 3 H), 7.35–7.43 (m, 2 H), 8.29–8.35 (m, 2 H), 8.90 (s, 1 H, NH), 10.89 (s, 1 H, OH); Mass: m/z 241.20; Anal. Calcd for $C_{15}H_{15}NO_2$: C, 74.67; H, 6.27; N, 5.81%. Found: C, 74.62; H, 6.29; N, 5.78%.

2-((3-(trifluoromethyl)phenyl)amino)benzoic acid (3c): Mp. 123–125 °C (lit. mp 125 °C)[21]; IR (KBr, cm^{-1}): 3452, 3105, 3001, 2975, 1643, 1575, 1484, 1311, 1265, 1145, 1085, 775, 670; ^{1}H NMR (DMSO-d6, 300 MHz): δ δ 7.13–7.20 (m, 2H), 7.60–7.69 (m, 2H), 7.57 (s, 1H), 8.2–8.32 (m, 3H), 9.02 (s, 1H, NH), 10.45 (s, 1H, OH); Mass: m/z 281; Anal. Calcd for $C_{14}H_{10}F_3NO_2$: C, 59.79; H, 3.58; N, 4.98%. Found: C, 59.75; H, 3.60; N, 4.96%.

General procedure for the synthesis of substituted 2-(phenylamino)benzamide (4a-b) Substituted 2-(phenylamino) benzoic acid (**3a-b**, 0.1 g, 0.38 mmol) was dissolved in DMF (4 mL) in a round bottom flask (25 mL) and the temperature was maintained at 0-5°C. To this solution EDC, HCl (0.0878 g, 0.45 mmol), and DMAP were successively added and the reaction mixture was stirred at 0-5°C till precipitate was obtained. Then HOBt (0.0702 g, 0.45 mmol) was added to the reaction mixture and the temperature is then maintained at 0-5°C. After 1 h, NH_4Cl (0.0245 g, 0.45 mmol) was successively added to the reaction mixture and the mixture was stirred at room temperature for hours. The reaction progress was monitored using TLC (chloroform:methanol, 9:1). After completion of the reaction, ice-cold water was added to the reaction mixture to obtain precipitate which was collected by filtration. The obtained crude product was subjected to purification technique column chromatography over silica gel (60–120 mesh) using chloroform:methanol as eluent to get the desired product (**4a-b**).

2-((3-chloro-2-methylphenyl)amino)benzamide (4a): Mp. 166 °C; IR (KBr, cm^{-1}): 3491, 3450, 3341, 3202, 2921, 1932, 1637, 1577, 1445, 1393, 1288, 1161, 1005, 801, 748, 637; ^{1} H NMR (DMSO-d6, 300 MHz): δ 3.50 (s, 3 H, CH_3), 5.17 (s, 2 H, NH_2), 6.55–6.59 (m, 2 H), 6.84 (t, J = 3 Hz, 1 H), 7.50–7.66 (m, 2 H), 7.72–7.74 (m, 2 H), 7.94–7.98 (m, 1 H); ^{13} C NMR (DMSO-d6, 75 MHz): δ 14 (1 C of CH_3), 112, 113, 116, 119, 127, 129, 130, 132, 134, 136, 172 (C = O); Mass: m/z 261.08; Anal. Calcd for $C_{14}H_{13}ClN_2O$: C, 64.50; H, 5.03; N, 10.74%. Found: C, 64.48; H, 5.04; N, 10.76%.

2-((2,3-dimethylphenyl)amino)benzamide (4b): Mp. 145 °C (lit. mp 140–141 °C)[22]; IR (KBr, cm^{-1}): 3489, 3447, 3374, 3209, 1635, 1578, 1505, 1447, 1287, 1149, 1072, 746, 636; ^{1}H NMR (DMSO-d6, 300 MHz): δ 2.21–2.27 (m, 6H, CH_3), 6.69 (t, J = 7.5 Hz, 1H), 6.78 (d, J = 8.7 Hz, 1H), 6.92 (d, J = 6.3 Hz, 1H), 7.03–7.108 (m, 1H), 7.23 (t, J = 7.8 Hz, 1H), 7.40 (s, 2H, NH_2), 7.68 (d, J = 9 Hz, 1H), 8.03 (s, 1H, NH), 9.90 (m, 1H); ^{13}C NMR (DMSO-d6, 75 MHz): δ 19, 21 (2C of CH_3), 118, 119, 126, 127, 133, 138, 149, 172 (C = O); Mass: m/z 241.12; Anal. Calcd for $C_{15}H_{16}N_2O$: C, 74.97; H, 6.71; N, 11.66%. Found: C, 74.98; H, 6.69; N, 11.67%.

General procedure for the synthesis of substituted 2-(phenylamino)benzoyl chloride (5a-c) Substituted 2-(phenylamino)benzoic acid (**3a-c**, 0.5 g, 1.7 mmol) was taken in a RB flasks also called round bottom flask (50 mL). To this thionyl chloride (0.15 mL, 2.1 mmol) was added slowly. The reaction mixture was then refluxed for 3 hours. The reaction progress was observed using TLC (chloroform:methanol, 9:1). After completion of the reaction, $SOCl_2$ was evaporated by *in vacuo*. The obtained crude product was subjected to column chromatography over silica gel (60–120 mesh) using hexane:ethyl acetate as eluent to get the desired product (**5a-c**).

2-((3-chloro-2-methylphenyl)amino)benzoyl chloride (5a): IR (KBr, cm^{-1}): 3282, 1627, 1596, 1573, 1499, 1238, 1198, 997, 755, 681; ^{1} H NMR (DMSO-d6, 500 MHz): δ 2.09 (s, 3 H, CH_3), 7.30–7.33 (m, 1 H), 7.34–7.42 (m, 1 H), 7.48–7.54 (m, 1 H), 7.74–7.82 (m, 1 H), 7.48–7.94 (d, J = 8.5 Hz, 1 H), 8.10 (d, J = 8.5 Hz, 1 H), 8.20 (d, J = 7.5 Hz, 1 H), 10.70 (s, 1 H, NH);); ^{13} C NMR (DMSO-d6, 75 MHz): δ 14 (1 C of CH_3), 118, 119, 125, 128, 132, 133, 135, 136, 140, 144, 168 (C = O); Mass: m/z 280; Anal. Calcd for $C_{14}H_{11}Cl_2NO$: C, 60.02; H, 3.96; N, 5.00%. Found: C, 60.00; H, 3.97; N, 5.01%.

2-((2,3-dimethylphenyl)amino)benzoyl chloride (5b): IR (KBr, cm^{-1}): 3283, 2919, 1625, 1599, 1567, 1538, 1467, 1267, 1193, 904, 754, 684; ^{1} H NMR (DMSO-d6, 500 MHz): δ 2.37–2.64 (m, 6 H, CH_3), 7.11 (d, J = 8 Hz, 1 H), 7.21–7.29 (m, 1 H), 7.71–7.76 (m, 1 H), 7.92 (d, J = 8.5 Hz, 1 H), 8.03 (d, J = 8 Hz, 1 H), 8.08–8.12 (m, 1 H), 8.19 (d, J = 8 Hz, 1 H), 10.47 (s, 1 H, NH); ^{13} C NMR (DMSO-d6, 75 MHz): δ 19, 21 (2 C of CH_3), 119, 120, 125, 127, 132, 133, 136, 138, 144, 168 (C = O); Mass: m/z 258.06; Anal. Calcd for $C_{15}H_{14}ClNO$: C, 69.37; H, 5.43; N, 5.39%. Found: C, 69.40; H, 5.41; N, 5.37%.

2-((3-(trifluoromethyl)phenyl)amino)benzoyl chloride (5c): IR (KBr, cm^{-1}): 3280, 3205, 3161, 3002, 2954, 1633, 1603, 1575, 1477, 1322, 1243, 1161, 1120, 1065, 833, 754, 675; ^{1}H NMR (DMSO-d6, 500 MHz): δ 7.32 (t, J = 7.5 Hz, 1H), 7.50 (d, J = 8.5 Hz, 1H), 7.55 (d, J = 8.5 Hz, 1H), 7.79 (t, J = 10 Hz, 2H), 7.87 (s, 1H), 8.24 (d, J = 8 Hz, 1H), 8.40 (d, J = 8.5 Hz, 1H), 12.04 (s, 1H, NH); ^{13}C NMR (DMSO-d6, 75 MHz): δ 115 (1C of CF_3), 119, 124, 125, 130, 132, 136, 142, 144, 168 (C = O); Mass: m/z 299; Anal. Calcd for $C_{14}H_9ClF_3NO$: C, 56.11; H, 3.03; N, 4.67%. Found: C, 56.14; H, 3.01; N, 4.65%.

Biological evaluation (*in vitro* studies)

Cell culture and drug treatment

Human cervical (SiHa) and breast (MCF-7, MDA-MB-231) cancer cells were procured from National Centre for Cell Sciences (NCCS), Pune, India. The cells were maintained in Dulbecco's Modified Eagle's medium (HiMedia, Mumbai) with 10% FBS (HiMedia, Mumbai), 100 U/mL penicillin, 100 mg/mL streptomycin and 250 ng/mL amphotericin B at 37°C in a humidified chamber consisting 5% CO_2 and 95% air. Cells were then incubated with standard trypsinization (Trypsin: 0.25%) at 85% confluency, and subcultured in ¼ ratio for routine maintenance and experimentation. Compound 3a-c, 4a-b and 5a-c were prepared in DMSO and exposed the cells for 48 h at final volume of 0.1% DMSO.

Cell proliferation assay

The inhibitory effect of selected drugs was measured by MTT assay [48]. Briefly, SiHa, MCF-7, and MDA-MB-231 cells were grown overnight in 96 well ELISA plate at density of $1.25\text{-}16 \times 10^3$ cells/well and treated with drug from 5 to 100 µM for 48 h. MTT (240 µg/ml) was added 4 h prior to end of incubation. Afterword's, medium was removed; acidified dimethyl sulfoxide (200 µL/well) was added, and incubated for 5 min at 37°C under shaking condition. Absorbance values at 570 nm was recorded using ELISA plate reader. Absorbance was recorded at 570 nm using ELISA reader and IC_{50} value was calculated from dose-response curves.

Prostaglandin E2 (PEG2) inhibitory assay

The PGE2 from culture medium of treated and untreated cells was estimated using a commercial kit (514,010; Cayman Chemical, MI, USA) and manufacture instruction was followed.

Cell cycle analysis

Siha cells (5×10^5/per dish) were seeded in 35 mm dish, left overnight and then treated with drugs. After 48 h, cells were harvested and fixed in 70% ice-cold ethanol, treated with solution consisting (50 µg/ml propidium iodide, 0.5% RNase A and 0.1% Triton X-100) for half an hours at 37 °C. Cells were analysed using BD FACScan Cell flow Cytometer (Becton Dickinson USA). Data acquisition and analysis was done using CellQuest software.

Trypan blue dye exclusion assay

SiHa cells were seeded at a density of 5×10^5 per well in 6 well plate, cultured for 12 h, and treated with drug from 5 to 100 µM for 96 h. Afterword, floating cells were transferred in tube, adherent cells were harvested, and mixed with floating cells before centrifugation. Cells were then stained with 0.4% trypan blue and enumerated under light microscope using hemocytometer. The live and dead cells were discriminated based on dye uptake.

Result

In silico studies

Computational ligand-target docking studies were successfully performed with 12,795 compounds using different databases. The COX-2 was minimized structure and stereochemical evaluation was performed through Ramachandran Plot indicated in Fig. 1a and b. Ramachandran plot showed the percentage of residues: 90.3 favoured regions, 9.2 additional allowed region, and 0.2 generously allowed region and 0.2 disallowed region, so the finding result by the Ramachandran plot represent the stereochemical stability of the minimized structure.

The docking results indicated three identified compounds (listed in Table 1) with a higher glide XP score than that of the COX-2 inhibitor. Glide pose viewer file was used for the

Table 1 Binding affinity and ADME prediction

S. No.	Title	XP Score (Schrodinger)	MMGBSA dG Bind Score	QPlog Po/w (-2.0 to 6.5)	QPPCaco (< 25 poor, > 50 great)	QPlogBB (-3.0 to 1.2)	QPlog KHSA (-1.5 to 1.5)
1.	ZINC5921547 Compound **4a**	-10.028	-64.042	-1.927	1231.017	-0.309	0.231
2.	ZINC48442590 compound **4b**	-10.007	-62.951	1.215	1162.003	-0.431	-0.758
3.	ZINC000039428234 Compound **5c**	-10.738	-63.204	-1.240	3072.101	0.337	0.571
4.	Reference compound (ID8)	-9.751	-60.190	0.273	1045.872	-0.266	-1.391

best conformation in the MMGBSA scoring function which accounts for the protein flexibility. The calculation of the "MMGBSA ΔG Bind" [dG] by the equation:

$$dGbind = E\_complex_{(minimized)} - (E\_ligand_{(minimized)} + E\_receptor_{(minimized)})$$

The higher affinity value was found in all selected compounds ZINC5921547 (**4a**), ZINC000039428234 (**5c**) and ZINC48442590 (**4b**) (-10.281, -10.738 and − 10.007 kcal/mol) with − 64.042, -63.204 and − 62.951 MMGBSA score compared with native ligand, it indicates the good-quality results as COX-2 inhibitor. The results were depicted in Table 1.

The protein-ligand docked structure and their interactions with the residues of the binding pocket were analyzed using protein-ligand interaction module. Figures 2, 3 and 4 portrays the interaction patterns between the main-chain or side-chain of the protein and compound(s). Hydrogen bonding between COX-2 receptor and ligand is represented by dashed lines in Figs. 2, 3 and 4.

QikProp wizard of Maestro-Schrodinger module and Molinspiration software were used to find out the ADMET and drug-likeness properties depicted in Tables 1 and 2. The pharmacokinetic parameters such as QPlogPo/w, QPPCaco, QPlogBB, and QPlog KHSA were analyzed. Several pharmacological properties of these compounds lie in falls satisfactorily in the acceptable range. The bioactive score is mentioned in Table 2.

The present results indicate that the bioactivity scores of the compounds were between − 5.0 and 0.0. The molecular descriptors and drug-likeliness properties of the ligands were also determined by molinspiration software. Based on the output we synthesized and evaluated their in vitro anticancer activity against three cancer cell lines.

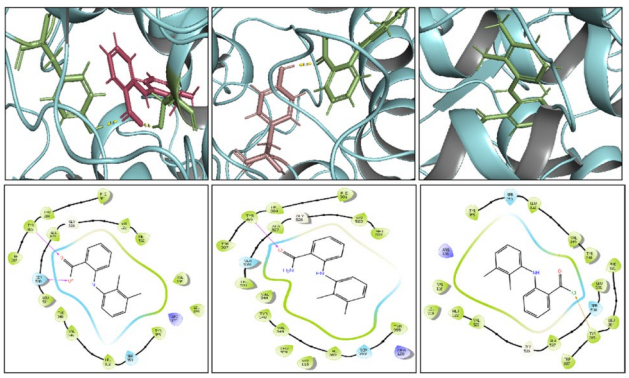

Fig. 2 Docking interaction between ligands (3b, 4b and 5b) and COX- protein target

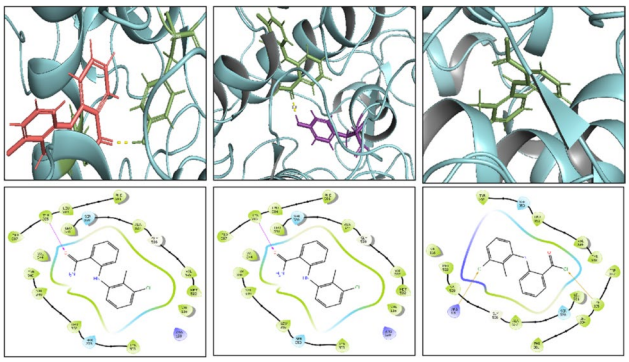

Fig. 3 Docking interaction between ligands (3a, 5a, and 4a) and COX- protein target

Chemistry evaluation

All the derived compounds were identified with ^{1}H NMR, FT-IR, mass spectroscopy and evaluated the anticancer activity by 3-(4,5 dimethylthiazol-2-yl)-2,5-diphenyl tetrazolium bromide (MTT) assay against MCF-7 (ER-positive), MDA-MB 231 (ER-negative), SiHa cell (Human cervical cancer cell).

The synthesis of intermediates and target compounds is outlined in Scheme 1. Substituted 2-(phenylamino)benzoic acid (**3a-c**) was prepared by a substitution reaction of 2-chlorobenzoic acid (**1**) and substituted aniline (**2**) dissolved in DMF. Cu was used as catalyst and CuO as co-catalyst to carry out the reaction to obtain the desired product **3a-c.** The obtained products **3a-c** were used as initial materials for the synthesis of products of series **4a-b** and **5a-c**. To obtain substituted 2-(phenylamino) benzamide (**4a-b**), 2-(phenylamino)benzoic acid was dissolved in DMF and in this solution EDC. HCl was added followed by the addition of DMAP. The reaction mixture

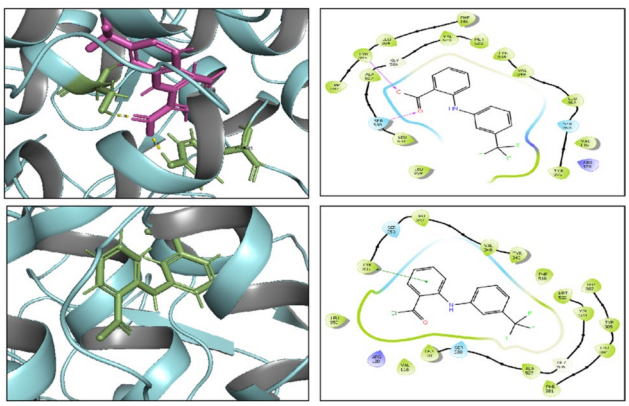

Fig. 4 Docking interaction between ligands (3c and 5c) and COX- protein target

Table 2 Molecular properties and bioactivity scores

S. No.	Compounds	Name	miLogP	TPSA(Å2)	Natoms	Molecular Weight	NON	nOHNH	violations	nrotb	Volume	GPCR Ligand	ICM	Kinase Inhibitor	NR	PI	EI
1.	ZINC5921547	**4a**	3.73	55.12	18	260.72	3	3	0	3	228.22	-0.35	-0.31	-0.08	-0.48	-0.54	-0.21
2.	ZINC48442590	**4b**	3.50	55.12	18	240.31	3	3	0	3	231.25	-0.31	-0.31	0.05	-0.50	-0.38	-0.13
3.	ZINC000039428234	**5c**	5.21	29.10	20	299.68	2	1	1	4	231.76	-0.29	-0.21	0.01	-0.23	-0.46	-0.26
4.	Reference compound (ID8)		4.77	49.33	18	241.29	3	2	0	3	227.98	-0.28	-0.20	-0.15	-0.16	-0.50	-0.10

was maintained at 0-5°C till the precipitate of EDU was obtained. The obtained precipitate dissolves on the addition of HOBt. Ammonium chloride was successively added to the reaction mixture. The mixture was allowed to stir at room temperature to obtain **4a-b**. For the synthesis of series **5a-c**, the substituted 2-(phenylamino)benzoic acid was reacted with thionyl chloride. The reaction was refluxed for 3 h to obtain substituted 2-(phenylamino)benzoyl chloride (5**a-c**). The obtained compounds **4a-b** and **5a-c** were confirmed by melting point, FT-IR, ^{1} H-NMR, and mass spectrometry. The presence of peaks indicates the formation of desired compounds.

Biological evaluation *(in vitro* studies)

Amide addition enhances antiproliferative activity in cancer cells

The anticancer effect of selected compounds on the growth of SiHa, MDA-MB-231 and MCF-7 were detected by MTT as described earlier. In the present experiment, cells were treated with parent compound (3a, 3b and 3c) and its derivative at 5, 10, 25, 50, and 100 µM for 24, 48, 72 and 96 h shown in Table 3. The dose-response curve was used to calculate the IC_{50} value, the drug concentration required to reduce cell proliferation by 50% against an untreated control. Cisplatin, one of the most effective metal-based anticancer agent, has been used as a standard reference. It is a FDA approved for the numerous cancer including breast ovarian, smack cell lung cancer, bladder, testicular, head and neck, cervical etc.[28, 49] which kills cancer cells by damaging DNA and inhibiting DNA synthesis.

The IC_{50} value for 3a in SiHa cells was found to 119.2 ± 6.7, 79.2 ± 6.1, 42.3 ± 3.4 and 35.9 ± 5.0 µM at 24, 48, 72 and 96 h respectively (Table 3). Interestingly, addition of amide group (4a) in 3a resulted in reduction in IC_{50} value to 101 ± 8.0, 64.6 ± 7.0, 36.9 ± 3.8 and 31 ± 1.5 µM at 24, 48, 72 and 96 h respectively (Table 3). Addition of amide group (4b) in parent compound (3b) also resulted reduction in IC_{50} value from 178.3 ± 14.9, 115.6 ± 9.1, 68.5 ± 4.7 and 56.5 ± 7.4 to 116.9 ± 7.5, 74 ± 8.1, 41.5 ± 4.8, and 21.5 ± 6.4 µM at 24, 48, 72 and 96 h respectively shown in Table 3. However, addition of chloride group (5a, 5b, 5c) in either 3a, or 3b or 3c, reduces the antiproliferative activity of the parent compound in SiHa cells (Table 3). These results are better than that of reference standard which recorded (6 ± 8.2, 14 ± 2.6, 13.3 ± 1.9 and 14.4 ± 1.1µM at 24, 48, 72 and 96 h respectively.

The MDA-MB-231 cell lines also demonstrated similar response. Addition of amide group (4a) in 3a reduces the IC_{50} value from 115.2 ± 11.8, 75.4 ± 8.4, 46.8 ± 8.1

Table 3 Comparative analysis of IC_{50} values of parent and amide, chloride derivatives in colorectal (SiHa cells) and breast (MCF-7 and MDA-MD-231 cells) cancer cell lines

Time (in hours)		3a	4a	5a	3b	4b	5b	3c	5c	Cisplatin
SiHa cells	24	119.2 ± 6.7	101 ± 8.0*	426.4 ± 37.2#	178.3 ± 14.9	116.9 ± 7.5*	377.3 ± 26.5#	96.3 ± 12.0	313.4 ± 27.8#	6 ± 8.2
	48	79.2 ± 6.1	64.6 ± 7.0	275.6 ± 15.1#	115.6 ± 9.1	74 ± 8.1*	250.8 ± 19.3#	59.5 ± 7.6	196 ± 15.7#	14 ± 2.6
	72	42.3 ± 3.4	36.9 ± 3.8	164.5 ± 12.6#	68.5 ± 4.7	41.5 ± 4.8*	144.4 ± 11.4#	29.8 ± 2.0	100.3 ± 7.3#	13.3 ± 1.9
	96	35.9 ± 5.0	31 ± 1.5	149.5 ± 12.6#	56.5 ± 7.4	21.5 ± 6.4*	119.7 ± 16.8#	34.1 ± 3.7	135.5 ± 8.2#	14.4 ± 1.1
MDA-MB-231	24	115.2 ± 11.8	94.7 ± 14.7	367.9 ± 28.5#	123.6 ± 10.3	99.3 ± 7.0*	177.6 ± 18.0#	124.4 ± 7.9	321.5 ± 28.7#	12 ± 3.1
	48	75.4 ± 8.4	59.8 ± 6.8	237.4 ± 24.6#	85.8 ± 7.4	64.2 ± 4.2*	117.7 ± 19.0	83.4 ± 7.8	224.8 ± 18.9#	24 ± 2.8
	72	46.8 ± 8.1	36.6 ± 2.7	151.9 ± 16.5#	51.6 ± 6.2	36.7 ± 5.2*	73.4 ± 7.9#	56.3 ± 7.0	137.5 ± 12.6#	10.6 ± 1.7
	96	51.9 ± 9.3	38 ± 3.9	177.9 ± 12.0#	58.2 ± 7.6	32.8 ± 4.5*	108.4 ± 9.4#	43.6 ± 2.7	110.6 ± 6.3#	19 ± 1.4
MCF-7 cells	24	166.6 ± 20.9	110.2 ± 13.0*	286.7 ± 25.2#	250.4 ± 19.3	150.9 ± 12.2*	407.9 ± 44.4#	174.8 ± 10.8	745.4 ± 61.9#	6.8 ± 1.9
	48	109.7 ± 10.0	72.9 ± 6.4*	184.7 ± 11.1#	161.9 ± 19.5	98.5 ± 5.9*	270.1 ± 36.3#	111.5 ± 6.6	513.3 ± 31.0#	18.5 ± 1.6
	72	64.3 ± 7.9	43.1 ± 2.5*	113.3 ± 8.9#	104.8 ± 11.4	64.8 ± 4.6*	185 ± 9.5#	54.4 ± 3.1	270.5 ± 17.5#	20.2 ± 1.3
	96	54 ± 5.6	35.5 ± 4.5*	95.7 ± 3.6#	88 ± 4.4	55.7 ± 7.8*	154.1 ± 21.1#	43.8 ± 5.4	211.2 ± 15.7#	20.8 ± 1.3

All experiments were conducted in triplicate, and the data expressed as the means ± SEM.

*$p < 0.05$ & #$p < 0.05$ as compared to respective parent compound

and 51.9 ± 9.3 to 94.7 ± 14.7, 59.8 ± 6.8 and 36.6 ± 2.7 µM at 24, 48, 72 and 96 h respectively (Table 3). Addition of amide group (4b) in 3b also reduces the IC_{50} value of 3b by ~ 43.6% at 96 h post-treatment (Table 3), superior to the reference standard that demonstrated an IC_{50} of 12 ± 3.1, 24 ± 2.8, 10.6 ± 1.7, 19 ± 1.4 µM at 24, 48, 72 and 96 h respectively. Addition of chloride group in all parent compounds enhances the IC_{50} value (Table 3).

Next, MCF-7 cell line was treated with selected compound to verify the consistency of selected compounds. Addition of amide group in either 3a or 3b, resulted in reduction in IC_{50} value (Table 3). The reduction in IC_{50} value after amide addition support the role of amide group in enchantment of anticancer efficacy, while addition of chloride group diminished the antiproliferative activity of parent compound under similar condition as clearly seen in Table 3. Regarding MCF-7, compounds **9a** and **11** expressed better antiproliferative activity than standard reference cisplatin (Table 3).

Prostaglandin E2 production

COX-2 is known to form the prostaglandin-E2 from arachidonic acid. Therefore PGE-2 was measured to test whether reduction in cell proliferation is due to PGE-2. In our observation, MDA-MB231 and SiHa cells produced higher PGE-2 than MCF-7 cells. The 3a, 4a, and 5a treatment at 50 µM for 48 resulted in reduction in PGE-2 level by 21.73%±0.86, 41.96%±2.14, and 6.37%±0.11 respectively against untreated control in SiHa cells (Fig. 5a). Similarly, 3b, 4b and 5b treatment at 50 µM resulted in decrease in PGE-2 level by 47.72%±1.95, 73.35%±2.79, and 5.22%±0.35 respectively at 48 h post-treatment against untreated control (Fig. 5b). Compound 5c induces the PGE2 against 3c at 48 h post-treatment (Fig. 5c). Our results indicate that addition of amide group enhances the potency of 3a, and 3b.

The 3a, 4a, and 5a at 50 µM resulted in reduction of PGE-2 level by 27.40%±1.14, 45.68%±2.63, 23.08%±2.39 respectively at 48 h against untreated control in MDA-MB-231 cells (Fig. 5d). The similar effect was observed with 3b, 3c and its derivatives namely 4b, 5b, and 5c (Fig. 5e and f).

The 3a, 4a, and 5a treatment to MCF-7 cells at 50 µM has shown to reduce the PGE-2 level by 7.57%±0.69, 31.81%±2.17, and 1.13%±0.05 respectively at 48 h post-treatment against untreated control (Fig. 5g). The 4b at 50 µM has shown to reduce the PGE2 level by 14.73%±0.76 at 48 h post-treatment against parent compound 3b (Fig. 5h). The 5c increases the PGE-2 level at 48 h against parent compound 3c (Fig. 5i).

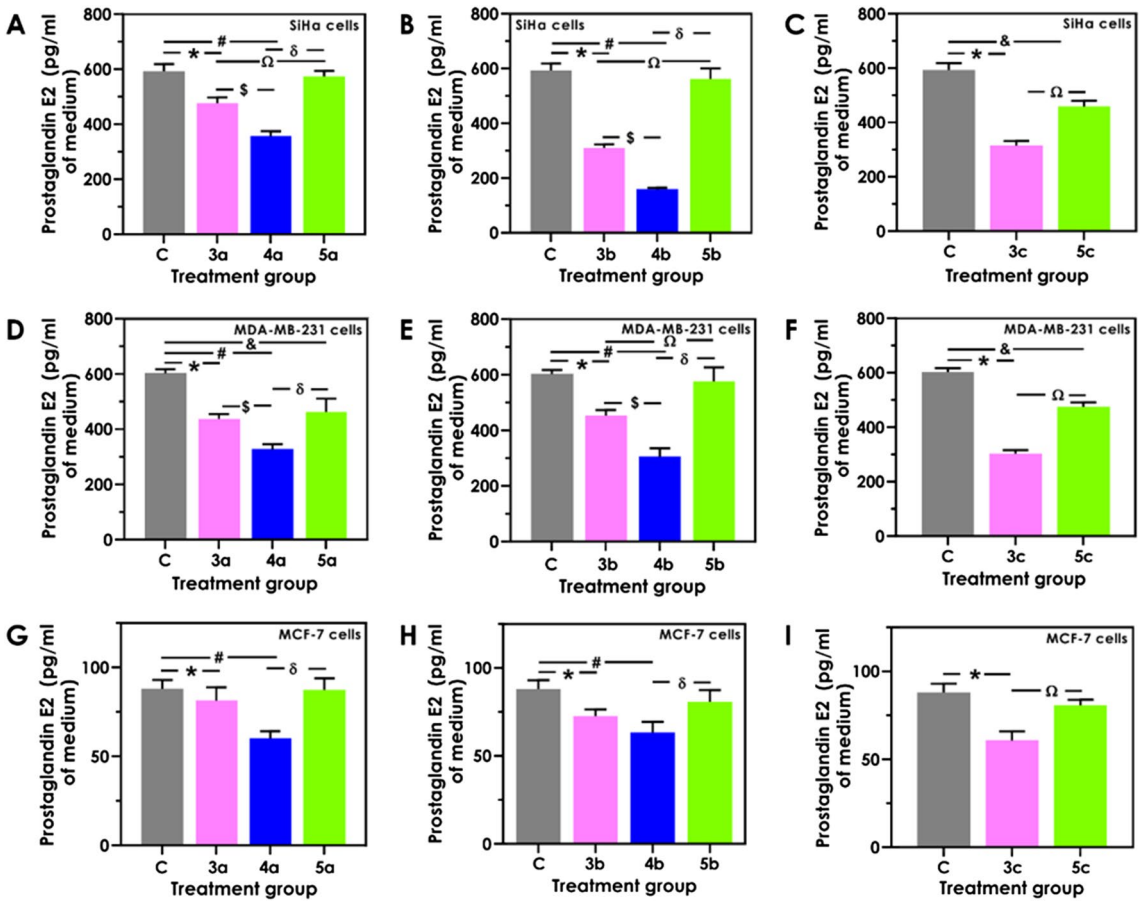

Fig. 5 (a-i) Effect of compounds under study on prostaglandin E2 in (a-c) SiHa, (d-f) MDA-MB231 and (g-i) MCF-7 cancer cell lines at 48 h post-treatment. Each bar denotes the mean ± Standard deviation SD. $n = 6$. *$p < 0.05$

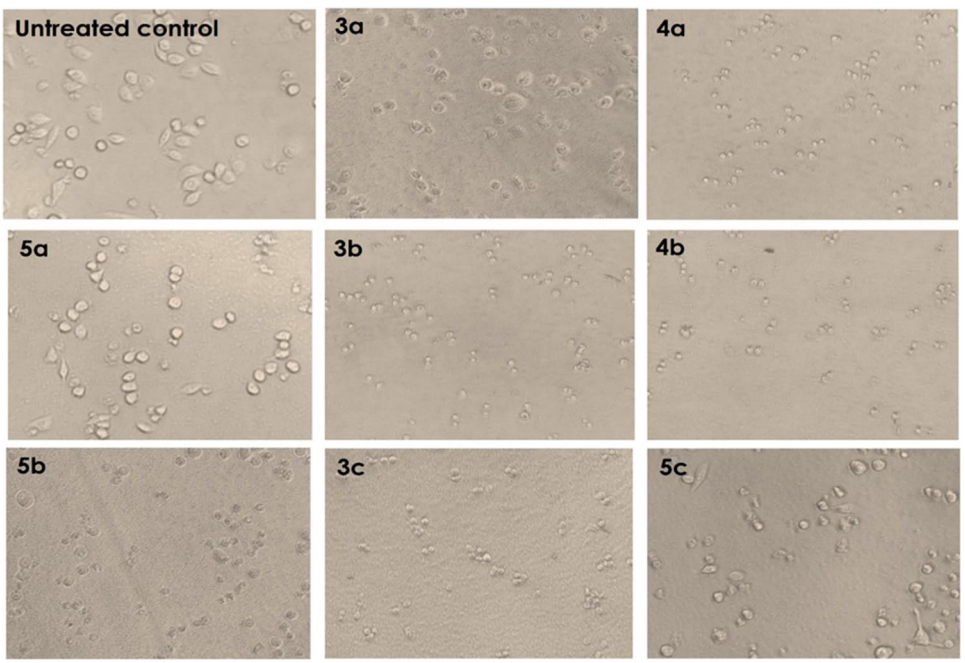

Fig. 6 Effects of compounds under study on SiHa cell morphology at 48 h post-treatment. (a) untreated control, (b-i) treatment with mentioned compound

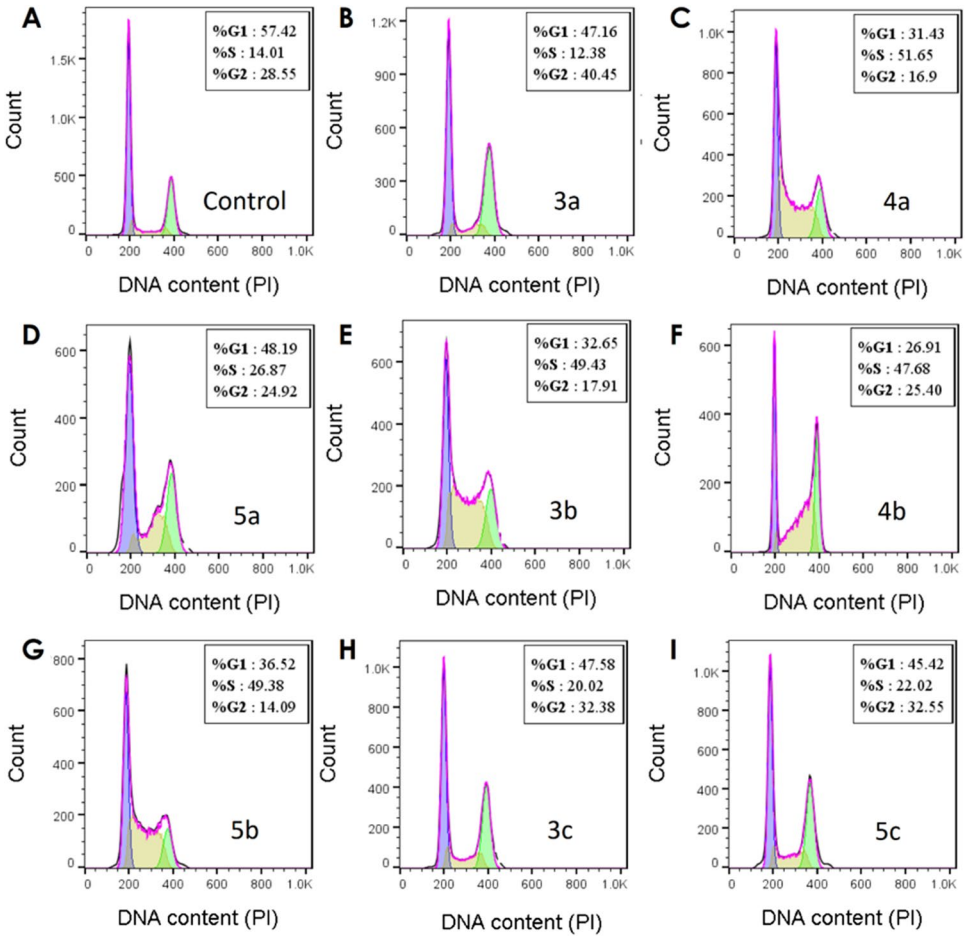

Fig. 7 Effects of compounds under study on cell cycle in SiHa cells at 48 h post-treatment. (a) untreated control, (b-i) treatment with mentioned compound

Effects of compound 3a, 3b, 3c and their derivatives on cell morphology

Morphological changes were recorded using microscope in SiHa cells, MCF-7 and MDA-MB-231 cells. For all untreated and treated cells, the images were observed at 48 h and the images were captured using a phase contrast light microscope. SiHa cells in the control group appeared phenotypically as a spindle-shaped and substantial in volume. It had larger nuclei, opaque and abundant cytoplasm (Fig. 6a). The cells were appeared to be firmly attached to the wall (Fig. 6a). The treatment with 3a, or 3b, or 3c or derivatives to SiHa cells at 50 µM for 48 h were result in acquiring irregular or round shape, and size reduction (Fig. 6a-i). The cell boundary was lost smooth appearance, and loose attachment of cells were also observed to the bottom (Fig. 6b-i). The 4a treated cells were smaller in size then 5a or 3a at 48 h post-treatment period (Fig. 6b-d). The similar effect was observed with 3b and its derivatives namely 4b&5b at 48 h post-treatment period (Fig. 6e-g). The 3c treated cells were smaller and lesser in volume than 5c treated SiHa cells (Fig. 6h and i). In present study, 4a and 4b were more potent than parent compounds. Moreover, reduction in cancer cell proliferation by compound utilized in present study probably an outcome of cell cycle blockage.

Effects of compound 3a, 3b, 3c, and their derivatives on cell cycle

The selected compounds in present study have shown most potent antiproliferative effect in SiHa cells. Therefore, we further studied the drug effect in SiHa cells for delineating the molecular mechanism behind antiproliferative effect. In present study, 4a and 5a have shown to activate G1/S cell cycle phase (Fig. 7c and d) against untreated control (Fig. 7a). Interestingly, 3a have shown to induces the cell cycle blockage at G2/M phase (Fig. 7b). 3b, 4b, and 5b at 50 µM have shown to induce the G1/S blockage at 48 h post-treatment (Fig. 7e-g). However, 4b was more efficient in inducing G1/S cell cycle halt than either 5b or 3b. The 3c and 5c has shown to arrest the cell cycle at G1/S and G2/M

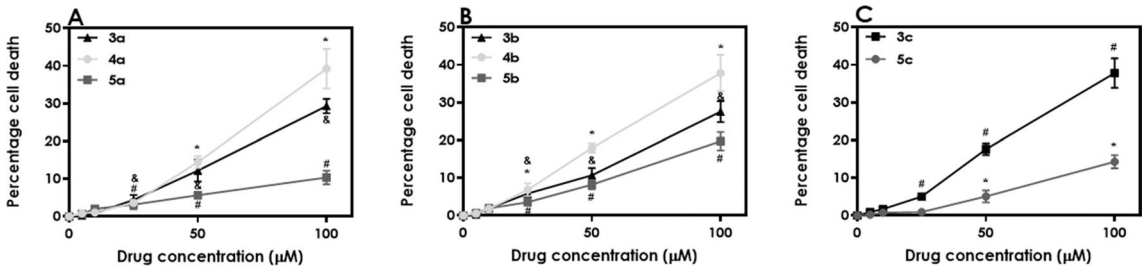

Fig. 8 Effects of compounds under study on SiHa cell death at 48 h post-treatment. Each data point represents the mean ± SD of $n = 6$. *$p < 0.05$

phase (Fig. 7h-i). However, no major difference in cell proportion at different cell cycle phase was observed between 3c and 5c.

Effects of compound 3a, 3b, 3c and derivatives on cancer cell death

Cell cycle blockage help in maintenance of genomic integrity, and failure to repair the damaged DNA result in cell death [31, 50]. Therefore, next we check whether reduction in cell proliferation is due to cell death or only cell cycle blockage. The cell cycle analysis for control and treated SiHa cells (Fig. 8) was analyzed using a flow cytometer. Compound 3a, 4a, and 5a treatment to SiHa cells at 100μM resulted in death of 29.32%±1.94, 39.24%±5.26, and 10.40%±1.80 cells respectively against untreated control at 48 h post-treatment (Fig. 8a). The 3b, 4b, and 5b treatment 100μM resulted in death of 27.57%±2.80, 37.80%±4.83, and 19.73%±2.44 SiHa cells respectively at 48 h post-treatment (Fig. 8b). The 3c and 5c at 100 μM has shown to reduce the cell proliferation by 37.80%±3.93, and 14.30%±1.74 respectively against untreated control at 48 h post-treatment (Fig. 8c). Our result shown that compound 4a and 4b showed improved anticancer activity.

Discussion

In addition, these cell lines are aggressive and invasive cervical and breast cancer (TNBC) are known to be resistant to several anti-cancer agents [31, 51]. In our computational and experimental studies, compound **4a, 4b and 5c** were selected as lead compounds for cancer treatment in humans. Based on the ΔG binding, **4a, 4b and 5c** have the higher affinity with COX-2 receptor when compared to reference compound (ID8), The hydrogen bond play a major role in protein folding, formation of protein secondary structure and molecular recognition [12, 23]. The bonding also provides stability of protein-ligand complex. Favourable hydrogen bond (H-bond) interactions, hydrophobic, cation-π, and π-π stacking and between ligand-protein residues at the binding site are encountered [52]. The H-bonding with key binding site residues Tyr385 and Ser 530 with 1.8 and 1.9Å were associated with compounds (**compound 4a, 4b, 3a-c, 5a**). These residues indicate responsible for holding the ligand in the binding pocket. The cation-π and interactions involving in compound **5b** and **5c** at Arg120 and protonated Tyr355 residue position respectively which helps in electrostatic contributions whereas π-π stacking non-covalent interaction involves in aromatic molecules compounds which plays key role in protein-ligand recognition and the organization of biomolecular structures [52]. Previous studies have reported that electrostatic interactions are preferred strongest interaction between drug and receptor [53]. There is no interaction observed in compound **5c**. Therefore, we suggest that these selected hits are better candidate to be used as the lead compounds to inhibit COX-2 activity.

These imply that the best compounds showed higher potency to inhibit the COX-2 enzyme. The Caco-2 is represented to be suitable mimics for the -blood barrier. However, the logBB (predicted brain/blood partition coefficient) and logKhsa values (prediction of binding to human serum albumin) lie within the acceptable range. The logP o/w provides the predicted octanol/water partition coefficient of the drug within the favourable range. The molinspiration chemoinformatics software was used for calculating the drug activity. It supports for calculation of molecular properties (Molecular weight, LogP, PSA, number of hydrogen bond donors and acceptors) and predict the bioactivity score (G-Protein Coupled Receptor ligands (GPCR), kinase inhibitors (KI), ion channel modulators (ICM), nuclear receptors (NR), protease inhibitor (PI), and enzyme inhibitor (EI) [54]. The present outcome demonstrated the molecular properties and bioactivity scores were found within the normal range. All the selective compounds follow Lipinski's rule. According to the rules, selected hits must not have a MV of > 500Da, must have a number of hydrogen bond donor (HBD) < 5 and acceptors (HBA) < 10, Log P value must have ≤ 5 and TPSA must have < 140Å [47, 55, 56]. In general, the bioactivity score is > 0.0, shows the compound is active; if the range

between −5.0 and 0.0, then it shows the moderately active, and if the score is < −5.0, then it is inactive. It is encouraging to note that three hits such as compounds **4a**, **4b**, and **5c** follow the rule, bioactivity, and molecular properties.

Prediction of anticancer drug potential of COX-2 receptor through computational approaches was further validated using in vitro studies. Our study demonstrated growth inhibition of cell increased with increasing the concentration of treatment. Overall, the desired compounds showed a significant ($p < 0.05$ *) cytotoxic activity. To check cytotoxic effect of compounds 3a, 4a, 5a, 3b, 4b, 5b, 3c and 5c on colorectal (SiHa cells) and breast (MCF-7 and MDA-MD-231 cells), MTT assay was performed. This technique is one of the reliable and sensitive indicators for measuring the cytotoxicity and evaluation of drug sensitivity on cancer cell line [31, 48, 57, 58]. Different drug doses (5, 10, 25, 50, and 100 µM) of selected compounds were chosen to detect the effective dose at minimum concentration. The cytotoxic effect of selected drugs was determined using this assay for assessing cell metabolic activity which indicates the dose and time dependant effect on cancer cells.

Prostaglandin-E2 has been found in several human malignancies and it promote the cancer cell proliferation by activating the cell signalling pathway involved in cell proliferation, angiogenesis, apoptotic inhibition etc. [59]. Present results showed a confirmation with the cell proliferation data, and indicting the role COX-2-PGE-2 axis in reduction of cancer cell proliferation [60]. The reduction in PGE2 level along with cell proliferation, indicate the role of PGE-2 in cancer cell proliferation [61].

Identified drugs are well-known inhibitors of cyclooxygenases, overexpressed in most tumors. With the aim to estimate the potential of the fenamate derivatives, their anticancer activity was evaluated in vitro. In present study, we observed that addition of the amide group in 3a, and 3b enhances the anticancer activity of the parent compound in selected cancer cell lines. Among all tested cell lines, SiHa cells was most sensitive, while MDA-MB-231 shown highest resistance. Present result indicates the reduction in cell proliferation is due to cell death, however role of cell cycle inhibition cannot be ruled out either. Our results also indicate that the association of the most potent antiproliferative activities with amide derivate (4a&4b) of 3a and 3b, which is confirmation with the earlier study [26]. The chloride derivates (5a&5b) of 3b and 3a had shown poor anticancer response. Compound 3a have shown to induce the breast cancer cell apoptosis by inducing the p53 and p21 [30]. However, role of induced cell cycle inhibition cannot ruled out either [62]. The 3b derivatives seemed to inhibit cell proliferation due to induction of ROS-dependent DNA damage [63]. Overall, it could be inferred from all these evidence that compounds ZINC5921547 and ZINC48442590 (**4a** and **4b**) could be a candidate exploring for the inhibition of the COX-2 protein.

Conclusion

In the present study, we identified three new compounds out of 12,795 compounds as novel and potent inhibitor of COX-2 using the 'similar target search' criterion. ZINC5921547, ZINC48442590, and ZINC000039428234 of the identified compound were studied to confirm the efficacy, safety profile, toxicity, and structural features required for binding. The identified compounds obeyed Lipinski's rule and were found better ADMET and drug-likeness properties. The identified compounds were synthesized and obtained in good yields. Among all compounds, compounds **4a** and **4b** have been observed to be more potent in reducing cell proliferation than parent compound in MCF-7, MDA-MB-231, and SiHa cell lines. Inhibition of the COX2-PGE2 axis was found to the major reason behind the anticancer activity. Compound **4a** and **4b** halt the cell cycle at the G1-S phase and induces cell death. In summary, ZINC5921547 and ZINC48442590 (**4a** and **4b**) were significantly more potent than compounds **3a**, and **3b**, and thus further studies on *in vivo* efficacy are required to develop them as new open possibilities of COX-2 inhibitor for cancer treatment and purpose.

Abbreviations COX-2: Cyclooxygenase-2; NSAIDs: Non-Steroid Anti-Inflammatory Drugs; PGE2: Prostaglandin E_2; PDB: Protein Data Bank; MMGBSA: Molecular Mechanics/Generalized Born Surface Area; ADMET: Adsorption, Distribution, Metabolism, Excretion, and Toxicity; FT-IR: Fourier-transform infrared spectroscopy; NMR: Nuclear magnetic resonance; MTT: (3-(4,5-Dimethylthiazol-2-yl); DMSO: Dimethylsulfoxide; DMF: Dimethylformamide

Author contribution Experimental design, data collection and analysis were performed by Ankita Sahu. The first draft of the manuscript was written by Ankita Sahu. Babita Veer conceived and planned the synthesis work and In vitro studies for anticancer agents were performed by Sumit Kumar. Dibyabhaba Pradhan, Ram Singh, Khalid Raza, Moshahid A. Rizvi and Arun Kumar Jain reviewed and edited the paper. Saurabh Verma conceptualized and supervised work. All authors read and approved the final manuscript.

Funding This work was supported by Indian Council of Medical Research (ICMR), India to Ankita Sahu under the scheme ICMR-Research Associateship (Grant No. 3/1/3/PDF(14)2016-HRD).

Data availability The datasets used and/or analysed during the current study are available from the corresponding author on reasonable request.

Declarations

Competing interests The authors declare that they have no competing interests.

References

1. Chandrasekharan NV, Simmons DL. The cyclooxygenases. Genome Biol. 2004;5: 241.
2. Clària J. Cyclooxygenase-2 biology. Curr Pharm Des. 2003;9:2177–90.
3. Chow LWC, Loo WTY, Toi M. Current directions for COX-2 inhibition in breast cancer. Biomed Pharmacother. 2005;59(Suppl 2):281–4.
4. Botting RM, Botting JH. The discovery of COX-2. In: Pairet M, van Ryn J, editors. COX-2 Inhibitors [Internet]. Basel: Birkhäuser; 2004 [cited 2023 Jan 3]. p. 1–13. Available from: https://doi.org/10.1007/978-3-0348-7879-1_1.
5. Sobolewski C, Cerella C, Dicato M, Ghibelli L, Diederich M. The role of Cyclooxygenase-2 in cell proliferation and cell death in human malignancies. Int J Cell Biol. 2010;2010:e215158 (Hindawi).
6. Müller-Decker K, Fürstenberger G. The cyclooxygenase-2-mediated prostaglandin signaling is causally related to epithelial carcinogenesis. Mol Carcinog. 2007;46:705–10.
7. Cervello M, Montalto G. Cyclooxygenases in hepatocellular carcinoma. World J Gastroenterol. 2006;12:5113–21.
8. Botting RM. Inhibitors of cyclooxygenases: mechanisms, selectivity and uses. J Physiol Pharmacol. 2006;57(Suppl 5):113–24.
9. Sahu A, Raza K, Pradhan D, Jain AK, Verma S. Cyclooxygenase-2 as a therapeutic target against human breast cancer: a comprehensive review. WIREs Mech Dis. 2023;15(3):e1596. https://doi.org/10.1002/wsbm.1596.
10. Kizhakkeppurath Kumaran A, Sahu A, Singh A, Aynikkattil Ravindran N, Chatterjee NS, Mathew S, Verma S. Proteoglycans in breast cancer, identification and characterization by LC-MS/MS assisted proteomics approach: a review. Proteomics Clin Appl. 2023;e2200046. https://doi.org/10.1002/prca.202200046.
11. Yadav MK, Sahu A, Anu, Kasturria N, Priyadarshini A, Gupta A et al. Clinical Applications of Protein-Based Therapeutics. In: Singh DB, Tripathi T, editors. Protein-based Therapeutics [Internet]. Singapore: Springer Nature; 2023 [cited 2023 Mar 10]. p. 23–47. Available from: https://doi.org/10.1007/978-981-19-8249-1_2.
12. Sahu A, Verma S, Varma M, Yadav MK. Impact of ErbB receptors and anticancer drugs against breast cancer: a review. Curr Pharm Biotechnol. 2022;23(6):787–802. https://doi.org/10.2174/1389201022666210719161453.
13. Gong Z, Huang W, Wang B, Liang N, Long S, Li W, et al. Interplay between cyclooxygenase–2 and microRNAs in cancer (review). Mol Med Rep Spandidos Publications. 2021;23:1–10.
14. Howe LR. Inflammation and breast cancer. Cyclooxygenase/prostaglandin signaling and breast cancer. Breast Cancer Res. 2007;9:210.
15. Ye Y, Wang X, Jeschke U. von Schönfeldt V. COX-2-PGE2-EPs in gynecological cancers. Arch Gynecol Obstet. 2020;301:1365–75.
16. Saeedian Moghadam E, Hamel E, Shahsavari Z, Amini M. Synthesis and anti-breast cancer activity of novel indibulin related diarylpyrrole derivatives. DARU J Pharm Sci. 2019;27:179–89.
17. Qureshi O, Dua A. COX Inhibitors. StatPearls [Internet]. Treasure Island (FL): StatPearls Publishing; 2023 [cited 2023 Apr 23]. Available from: http://www.ncbi.nlm.nih.gov/books/NBK549795/.
18. Kolawole OR, Kashfi K. NSAIDs and cancer resolution: new paradigms beyond cyclooxygenase. Int J Mol Sci. 2022;23:1432 (Multidisciplinary Digital Publishing Institute).
19. Mosalpuria K, Hall C, Krishnamurthy S, Lodhi A, Hallman DM, Baraniuk MS, et al. Cyclooxygenase-2 expression in non-metastatic triple-negative breast cancer patients. Mol Clin Oncol. 2014;2:845–50.
20. Tian J, Wang V, Wang N, Khadang B, Boudreault J, Bakdounes K, et al. Identification of MFGE8 and KLK5/7 as mediators of breast tumorigenesis and resistance to COX-2 inhibition. Breast Cancer Res. 2021;23:23.
21. Sahu A, Pradhan D, Raza K, Qazi S, Jain AK, Verma S. *In silico* library design, screening and MD simulation of COX-2 inhibitors for anticancer activity. In: 12th International Conference on Bioinformatics and Computational Biology. EPiC Series in Computing. EPiC Series in Computing. 2020;70:21–32.
22. Bajorath J. Computer-aided drug discovery. F1000Res [Internet]. 2015;4:1–8 [cited 2018 Oct 29]. Available from: https://www.ncbi.nlm.nih.gov/pmc/articles/PMC4756805/. https://doi.org/10.12688/f1000research.6653.1.
23. Kitchen DB, Decornez H, Furr JR, Bajorath J. Docking and scoring in virtual screening for drug discovery: methods and applications. Nat Rev Drug Discov. 2004;3:935–49.
24. Jiang H, Zeng B, Chen G-L, Bot D, Eastmond S, Elsenussi SE, et al. Effect of non-steroidal anti-inflammatory drugs and new fenamate analogues on TRPC4 and TRPC5 channels. Biochem Pharmacol. 2012;83:923–31.
25. Bindu S, Mazumder S, Bandyopadhyay U. Non-steroidal anti-inflammatory drugs (NSAIDs) and organ damage: a current perspective. Biochem Pharmacol. 2020;180: 114147.
26. Mathew B, Hobrath JV, Lu W, Li Y, Reynolds RC. Synthesis and preliminary assessment of the anticancer and Wnt/β-catenin inhibitory activity of small amide libraries of fenamates and profens. Med Chem Res. 2017;26:3038–45.
27. Li J, Mansmann UR. Modeling of non-steroidal anti-inflammatory drug effect within signaling pathways and miRNA-regulation pathways. PLOS ONE. 2013;8:e72477 (Public Library of Science).
28. El-Sheikh A, Khired Z. Interactions of analgesics with cisplatin: modulation of anticancer efficacy and potential organ toxicity. Med (Kaunas). 2021;58:46.
29. Moris D, Kontos M, Spartalis E, Fentiman IS. The role of NSAIDs in breast cancer prevention and relapse: current evidence and future perspectives. Breast Care (Basel). 2016;11:339–44.
30. Kim H-J, Cho S-D, Kim J, Kim S-J, Choi C, Kim J-S, et al. Apoptotic effect of tolfenamic acid on MDA-MB-231 breast cancer cells and xenograft tumors. J Clin Biochem Nutr. 2013;53:21–6.
31. Razak NA, Abu N, Ho WY, Zamberi NR, Tan SW, Alitheen NB, et al. Cytotoxicity of eupatorin in MCF-7 and MDA-MB-231 human breast cancer cells via cell cycle arrest, anti-angiogenesis and induction of apoptosis. Sci Rep Nat Publishing Group. 2019;9:1514.
32. Klose C, Straub I, Riehle M, Ranta F, Krautwurst D, Ullrich S, et al. Fenamates as TRP channel blockers: mefenamic acid selectively blocks TRPM3. Br J Pharmacol. 2011;162:1757–69.
33. Čeponytė U, Paškevičiūtė M, Petrikaitė V. Comparison of NSAIDs activity in COX-2 expressing and non-expressing 2D and 3D pancreatic cancer cell cultures. Cancer Manag Res. 2018;10:1543–51.
34. Elmaaty AA, Darwish KM, Chrouda A, Boseila AA, Tantawy MA, Elhady SS, et al. In Silico and *in vitro* studies for benzimidazole anthelmintics repurposing as VEGFR-2 antagonists: novel mebendazole-loaded mixed micelles with enhanced dissolution and anticancer activity. ACS Omega. 2022;7:875–99.
35. Laskowski RA, MacArthur MW, Moss DS, Thornton JM. PROCHECK: a program to check the stereochemical quality of protein structures. J Appl Cryst. 1993;26:283–91.
36. Sterling T, Irwin JJ. ZINC 15 – ligand Discovery for everyone. J Chem Inf Model. 2015;55:2324–37.
37. Ayers M, ChemSpider. The free chemical database. Reference reviews. 2012;26(7):45–6.
38. Pence HE, Williams A. ChemSpider: an online chemical information resource. J Chem Educ. 2010;87:1123–4.

39. Gilson MK, Liu T, Baitaluk M, Nicola G, Hwang L, Chong J. BindingDB in 2015: a public database for medicinal chemistry, computational chemistry and systems pharmacology. Nucleic Acids Res. 2016;44:D1045-1053.
40. Sastry GM, Adzhigirey M, Day T, Annabhimoju R, Sherman W. Protein and ligand preparation: parameters, protocols, and influence on virtual screening enrichments. J Comput Aided Mol Des. 2013;27:221–34.
41. Shelley JC, Cholleti A, Frye LL, Greenwood JR, Timlin MR, Uchimaya M. Epik: a software program for pKaprediction and protonation state generation for drug-like molecules. J Comput Aided Mol Des. 2007;21:681–91.
42. Friesner RA, Banks JL, Murphy RB, Halgren TA, Klicic JJ, Mainz DT, et al. Glide: a new approach for rapid, accurate docking and scoring. 1. Method and assessment of docking accuracy. J Med Chem. 2004;47:1739–49.
43. Friesner RA, Murphy RB, Repasky MP, Frye LL, Greenwood JR, Halgren TA, et al. Extra precision glide: docking and scoring incorporating a model of hydrophobic enclosure for protein-ligand complexes. J Med Chem. 2006;49:6177–96.
44. Genheden S, Ryde U. The MM/PBSA and MM/GBSA methods to estimate ligand-binding affinities. Expert Opin Drug Discov. 2015;10:449–61.
45. Norinder U, Bergström CAS. Prediction of ADMET properties. ChemMedChem. 2006;1:920–37.
46. Cheng F, Li W, Liu G, Tang Y. *In silico* ADMET prediction: recent advances, current challenges and future trends. Curr Top Med Chem. 2013;13:1273–89.
47. Lipinski CA. Rule of five in 2015 and beyond: target and ligand structural limitations, ligand chemistry structure and drug discovery project decisions. Adv Drug Deliv Rev. 2016;101:34–41.
48. Tolosa L, Donato MT, Gómez-Lechón MJ. General cytotoxicity assessment by means of the MTT assay. Methods Mol Biol. 2015;1250:333–48.
49. Florea A-M, Büsselberg D. Cisplatin as an anti-tumor drug: cellular mechanisms of activity, drug resistance and induced side effects. Cancers (Basel). 2011;3:1351–71.
50. Campos A, Clemente-Blanco A. Cell cycle and DNA repair regulation in the damage response: protein phosphatases take over the Reins. Int J Mol Sci. 2020;21:446 (Multidisciplinary Digit Publishing Inst).
51. Kwon S, Yang W, Moon D, Kim KS. Comparison of cancer cell elasticity by cell type. J Cancer. 2020;11:5403–12.
52. Brylinski M. Aromatic interactions at the ligand-protein interface: implications for the development of docking scoring functions. Chem Biol Drug Des. 2018;91:380–90.
53. Labute P. The generalized Born/volume integral implicit solvent model: estimation of the free energy of hydration using London dispersion instead of atomic surface area. J Comput Chem. 2008;29:1693–8.
54. Grob S. Molinspiration cheminformatics free web services. 2021. http://www.molinspiration.com.
55. Lipinski CA. Drug-like properties and the causes of poor solubility and poor permeability. J Pharmacol Toxicol Methods. 2000;44:235–49.
56. Lipinski CA. Lead- and drug-like compounds: the rule-of-five revolution. Drug Discov Today Technol. 2004;1:337–41.
57. Ashourpour M, Mostafavi Hosseini F, Amini M, Saeedian Moghadam E, Kazerouni F, Arman SY, et al. Pyrazole derivatives induce apoptosis via ROS Generation in the Triple negative breast Cancer cells, MDA-MB-468. Asian Pacific Journal of Cancer Prevention. Volume 22. West Asia Organization for Cancer Prevention (WAOCP),; 2021. pp. 2079–87. APOCP's West Asia Chapter.
58. Asghari N, Houshmand S, Rigi A, Mohammadzadeh V, Piri Dizaj M, Mousavian Hiagh ZS. PEGylated cationic nano-niosomes formulation containing herbal medicine curcumin for drug delivery to MCF-7 breast cancer cells. Eurasian Chem Commun. 2023;5:556–68 (Sami Publishing Co (SPC)).
59. Finetti F, Travelli C, Ercoli J, Colombo G, Buoso E, Trabalzini L. Prostaglandin E2 and cancer: insight into tumor progression and immunity. Biology (Basel). 2020;9(12):434. https://doi.org/10.3390/biology9120434.
60. Greenhough A, Smartt HJM, Moore AE, Roberts HR, Williams AC, Paraskeva C, et al. The COX-2/PGE2 pathway: key roles in the hallmarks of cancer and adaptation to the tumour microenvironment. Carcinogenesis. 2009;30:377–86.
61. Park JY, Pillinger MH, Abramson SB. Prostaglandin E2 synthesis and secretion: the role of PGE2 synthases. Clin Immunol. 2006;119:229–40.
62. Sutphin RM, Connelly SF, Lee CM, Sankpal UT, Eslin D, Khan M, et al. Anti-leukemic response of a NSAID, tolfenamic acid. Target Oncol. 2014;9:135–44.
63. Altay A, Caglar S, Caglar B, Sahin ZS. Novel silver(I) complexes bearing mefenamic acid and pyridine derivatives: synthesis, chemical characterization and in vitro anticancer evaluation. Inorg Chim Acta. 2019;493:61–71.